NASA Technical Memorandum 104324

Design and Integration of an Actuated Nose Strake Control System

Bradley C. Flick, Michael P. Thomson, Victoria A. Regenie,
Keith D. Wichman, Joseph W. Pahle, and Michael R. Earls

October 1996

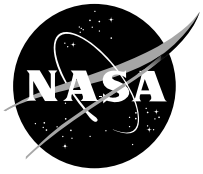

National Aeronautics and
Space Administration

NASA Technical Memorandum 104324

Design and Integration of an Actuated Nose Strake Control System

Bradley C. Flick, Michael P. Thomson, Victoria A. Regenie,
Keith D. Wichman, Joseph W. Pahle, and Michael R. Earls
NASA Dryden Flight Research Center
Edwards, California

1996

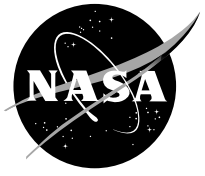

National Aeronautics and
Space Administration

Dryden Flight Research Center
Edwards, California 93523-0273

DESIGN AND INTEGRATION OF AN ACTUATED NOSE STRAKE CONTROL SYSTEM

Bradley C. Flick, Michael P. Thomson, Victoria A. Regenie
Keith D. Wichman, Joseph W. Pahle, Michael R. Earls
NASA Dryden Flight Research Center
Edwards, California

ABSTRACT

Aircraft flight characteristics at high angles of attack can be improved by controlling vortices shed from the nose. These characteristics have been investigated with the integration of the actuated nose strakes for enhanced rolling (ANSER) control system into the NASA F-18 High Alpha Research Vehicle. Several hardware and software systems were developed to enable performance of the research goals. A strake interface box was developed to perform actuator control and failure detection outside the flight control computer. A three-mode ANSER control law was developed and installed in the Research Flight Control System. The thrust-vectoring mode does not command the strakes. The strakes and thrust-vectoring mode uses a combination of thrust vectoring and strakes for lateral–directional control, and strake mode uses strakes only for lateral–directional control. The system was integrated and tested in the Dryden Flight Research Center (DFRC) simulation for testing before installation in the aircraft. Performance of the ANSER system was monitored in real time during the 89-flight ANSER flight test program in the DFRC Mission Control Center. One discrepancy resulted in a set of research data not being obtained. The experiment was otherwise considered a success with the majority of the research objectives being met.

NOMENCLATURE

ADC	analog-to-digital converter
AIL	aileron
ANSER	actuated nose strake for enhanced rolling
AOA	angle of attack
AUTO	automatic
BADSA	backup airdata sensor assembly
BIT	built-in test
BRT	brightness
CAS	control augmentation system
cmd	command
CONT	contrast

DAC	digital-to-analog converter
DDI	digital display indicator
DEGD	degrade
DFRC	Dryden Flight Research Center, Edwards, California
DPRAM	dual-port random access memory
EEPROM	electrically erasable programmable read-only memory
EHV	electrohydraulic valve
FCC	flight control computer
FCS	flight control system
G	gain set
g	acceleration due to gravity, 32.2 ft/sec^2
GN	gain
GND	ground
HARV	High Alpha Research Vehicle
HATP	High-Angle-of-Attack Technology Program
HUD	head-up display
h	altitude, ft
INS	Inertial Navigation System
I/O	input–output
L	left
LaRC	Langley Research Center, Hampton, Virginia
LEF	leading-edge flap
LVDT	linear variable displacement transformer
M	Mach number
MC	mission computer
MCC	Mission Control Center
MNVR	maneuver
NASA	National Aeronautics and Space Administration
N_y	lateral acceleration, g
N_z	normal acceleration, g
OAV	onboard augmented vehicle
OBES	onboard excitation system
P	pitch
PAL	programmable array logic

PDS	parameter display system
PLA	power lever angle, deg
Pos	position
PROC	processor
R	roll
RAV	remotely augmented vehicle
RFCS	research flight control system
ROM	read-only memory
Rt	right
RUD	rudder
S	strake mode
SIB	strake interface box
SOV	shutoff valve
STAB	stabilator
STV	strakes and thrust-vectoring mode
SV1	servovalve 1
SV2	servovalve 2
TD	trail damped
TEF	trailing-edge flap
TH1	threshold
TV	thrust-vectoring mode
TVCS	thrust-vectoring control system
TVV	thrust-vectoring vane
TVVS	thrust-vectoring vane system
V	volts
Vdc	volts, direct current
VME	Versa Module Eurocard
Vrms	volts root-mean-square
WOW	weight on wheels
Y	yaw
$\dot{\alpha}$	angle of attack rate, deg/sec
β	angle of sideslip, deg
$\dot{\beta}$	angle of sideslip rate, deg/sec
Σ	sum

INTRODUCTION

The F-18 High Alpha Research Vehicle (HARV) flown at Dryden Flight Research Center (DFRC), Edwards, California, is a flight test platform for the High-Angle-of-Attack Technology Program (HATP). One HATP objective involves improving aircraft controllability and agility at high angles of attack (ref. 1). The first phase of the program investigated high-angle-of-attack aerodynamics in a baseline F-18 configuration. During the second phase, the aircraft was modified by integrating a research flight control system (RFCS) with the basic F-18 control system. The RFCS allows various flight control laws to be flown. The standard F-18 system provides input, output, redundancy management, and safe backup for the RFCS. A thrust-vectoring (TV) system was also added to the HARV. This modification includes the addition of TV vanes to deflect engine exhaust for high-angle-of-attack maneuvering.

The third and final phase investigated an alternate control methodology for high-angle-of-attack maneuvering. Langley Research Center (LaRC), Hampton, Virginia, developed a system to apply forcing moments to the nose of the aircraft by controlling the vortices shed from the nose at high angles of attack (ref. 2). The actuated nose strake for enhanced rolling (ANSER) system consists of two actuated control surfaces installed in a specially constructed radome (fig. 1).

EC96-43598-11

Figure 1. The F-18 HARV.

The DFRC integrated the ANSER system with the RFCS and aircraft systems and conducted the flight research to accomplish these tasks. Several hardware and software systems were designed and developed. This paper describes the systems developed to integrate the ANSER into the aircraft and integration testing. Some of the technologies developed to enable accomplishment of the research objectives are discussed. Use of trade names or names of manufacturers in this

document does not constitute an official endorsement of such products or manufacturers, either expressed or implied, by the National Aeronautics and Space Administration.

SYSTEM OVERVIEW

The ANSER installation was designed to use full actuator authority to provide 90° of strake deflection (fig. 1). These strakes are commanded independently by control laws residing in the RFCS computers with two independent channels controlling each strake. The RFCS computers are F-18 flight control computers modified by the addition of a second processor running parallel and sharing data with the main processor. Figure 2 shows a top-level diagram of the control system. The RFCS software is written in Ada and cross-compiled on a UNIX®-based workstation. The compiled software is then downloaded to the RFCS.

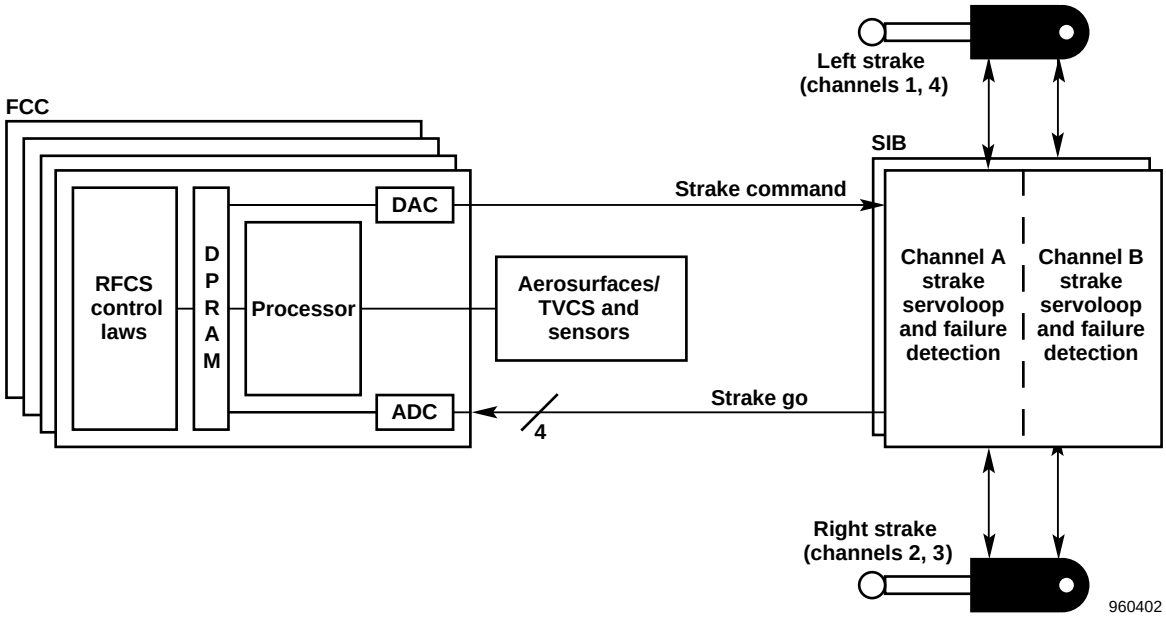

Figure 2. The F-18 HARV ANSER control system.

The RFCS control laws can be engaged with weight on the wheels or when the aircraft is in a predefined Mach number, M, and altitude, h, flight envelope (15,000 ft < h < 45,000 ft, M < 0.7) by first arming the system with a cockpit-mounted toggle switch, then engaging with a push button on the control stick. Research objectives required operation of the strakes both in conjunction with and independent of the TV system, resulting in a multimode control law implementation. Upon engagement, the RFCS defaults to TV mode in which the strakes are commanded closed at all times. Strakes and thrust-vectoring (STV) and strake (S) modes are selectable via a push button on the digital display indicator (DDI).

®UNIX is a registered trademark of UNIX System Laboratories, Inc.

Unlike the other control surfaces, which are only commanded by the RFCS control laws while RFCS is engaged (ref. 3), the strakes are commanded by the RFCS control laws at all times through previously unused analog outputs. Similarly, actuator control for the conventional surfaces and TV vanes are performed by the flight control computer (FCC); meanwhile, the strakes are controlled by an external interface box.

HARDWARE DESIGN AND IMPLEMENTATION

Control of the strakes is performed by two electrically controlled, hydraulically powered servoactuators. These actuators are F-18 aileron actuator servovalves mounted to a longer, narrower main piston and cylinder. The strake actuator piston length is 5.68 in. ±0.05 in. in place of the 4.38 in. ±0.05 in. as installed on the standard actuator. The actuators are dual redundant. Either channel can drive the surface. Hydraulic supply is single string to both actuators. The hydraulics are plumbed to the gun hydraulic quick disconnect located in the nose barrel section of the aircraft.

Integration of the strake actuators with the FCS required the addition of actuator control loop closure and failure detection for the strake actuators. These functions are normally performed in the FCC software. However, insufficient FCC input–output (I/O) availability required implementation of these functions external to the FCC in a strake interface box (SIB). The RFCS strake commands are passed through a previously unused digital-to-analog converter (DAC) to the servoloop located in the SIB. The servoloop performs loop closure and sends a rate command to the actuator. Several control loop signals are monitored by the failure-detection circuitry, which sends a go/no go signal back to the RFCS via a previously unused analog-to-digital converter (ADC). If a no go signal is received, the RFCS automatically reverts to TV mode and commands the strake to close. The SIB contains two independent channels of actuator control and failure detection. Each SIB channel controls one channel of each actuator (fig. 2).

Because the actuators used to drive the strakes are modified F-18 actuators, spare servoloop circuit cards were modified for use in the SIB to reduce manufacturing costs for a newly designed card. These cards were originally designed for use in the thrust-vectoring vane (TVV) system. The servoloop cards contain three identical servoloops of which two were used for the strake system. Figure 3 shows a block diagram of the servoloop board. Servoloop integrity is monitored by comparing the command output to that of a servoloop model which runs in parallel with the actual servoloop. A miscompare results in generation of a failure signal which is passed to the failure-detection circuitry for system monitoring. In addition to the servoloop function, this card performs all signal conditioning necessary for signal usage by the failure-detection logic. The card also receives discrete information back from the failure-detection logic for use in the servovalve and shutoff valve driver circuitry. This card was originally intended to be addressed by the FCC, so minor modifications were made to permanently enable discrete I/O of the board. A 1.8432-MHz clock was also added to these boards to trigger a programmable array logic (PAL) integrated circuit.

The software failure detection routines implemented in the FCC for the TVV actuators were also implemented in the SIB for the strake system. These routines include a comparison of servovalve command current to servovalve position (fig. 4), a main ram linear variable displacement

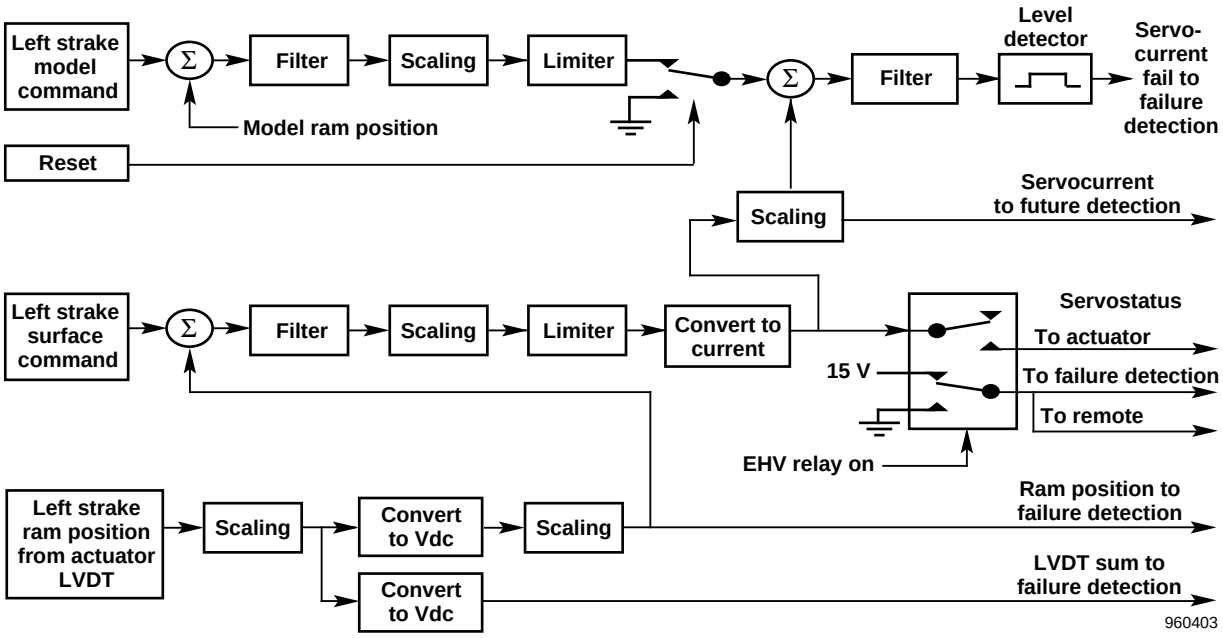

Figure 3. Servoloop card.

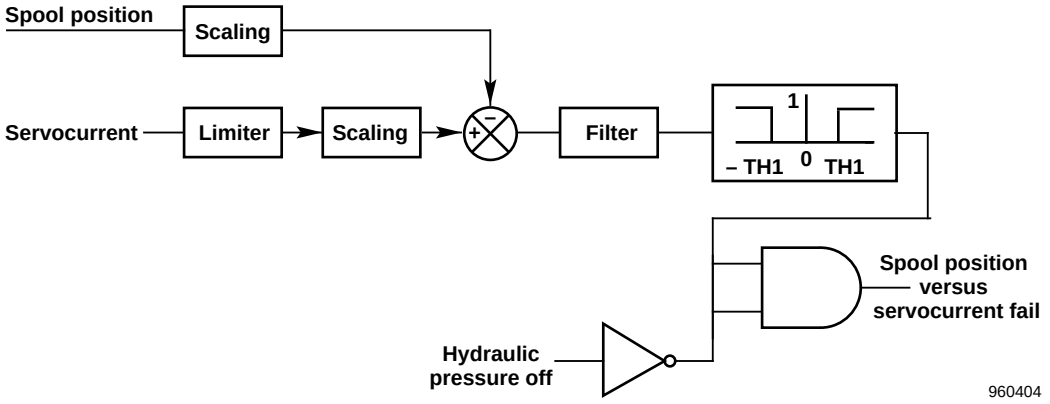

Figure 4. Spool position versus servocurrent test.

transformer (LVDT) monitor (fig. 5), and a hydraulic pressure sensor monitor (fig. 6). Each of these tests generates a discrete signal which is passed back to the servoloop board for actuator shut-off valve and servovalve relay control. Figure 7 shows the relay control logic. As shown in figure 7, the failures would self-reset upon clearing with no manual reset capability. A built-in test (BIT) circuit was integrated into the design which sequentially interrupts various actuator control signals to verify the integrity of the failure-detection circuitry (fig. 8). Because a processor was not designed into the system, monitoring of the BIT was performed manually in the Mission Control Center (MCC) before each flight. Although not as efficient as an automatic system, this approach proved adequate for this system.

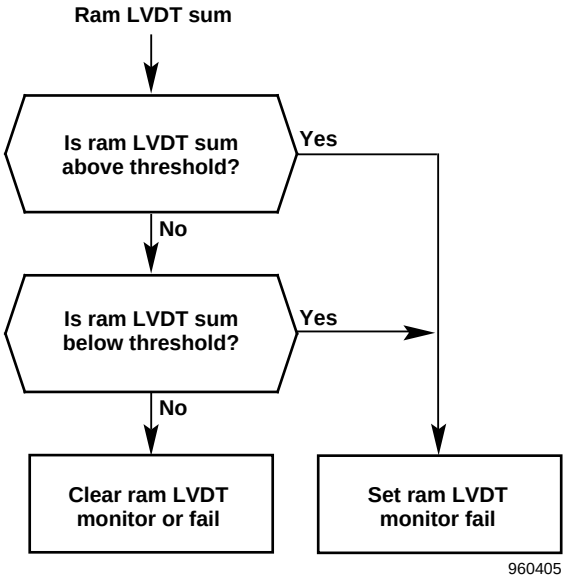

Figure 5. Ram LVDT monitor.

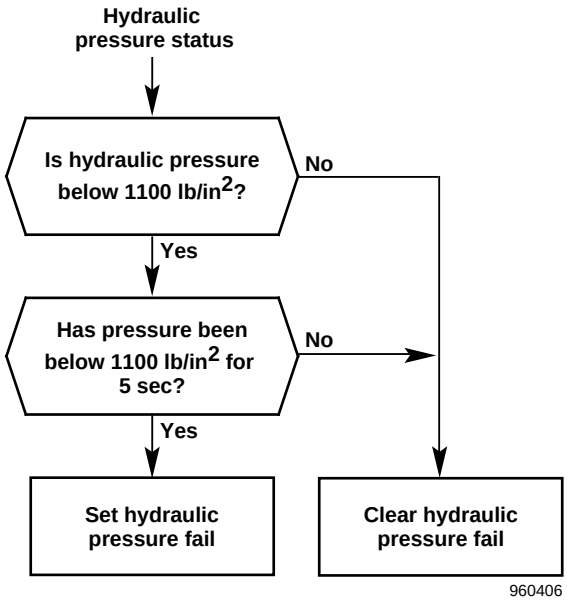

Figure 6. Hydraulic pressure monitor.

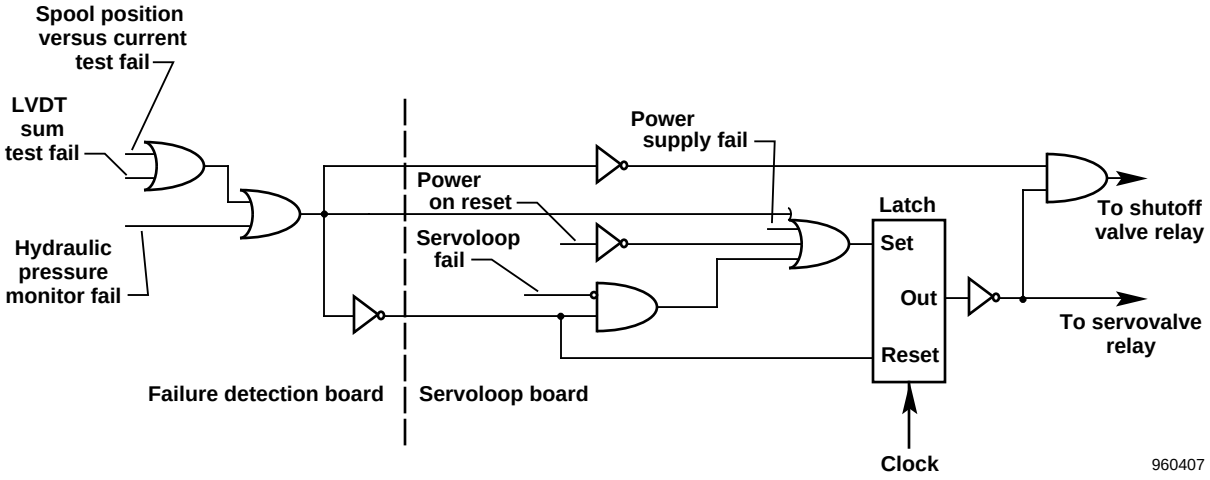

Figure 7. Failure logic.

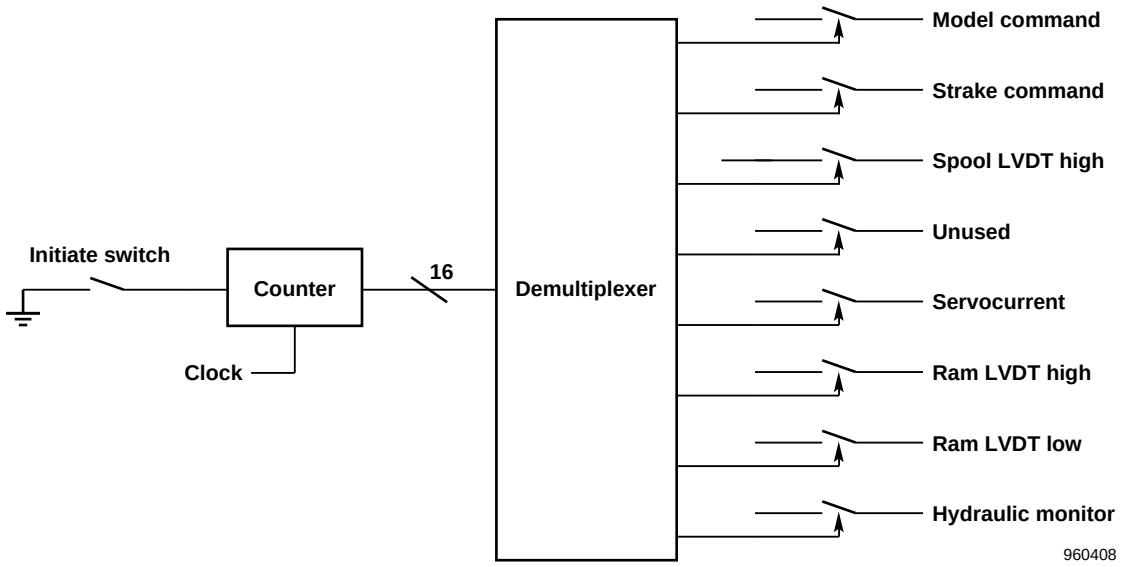

Figure 8. The ANSER built-in test.

The SIB is powered by two independent power supply modules which regulate aircraft 28 Vdc and convert it to ±15 Vdc, 5 Vdc, and 8 Vrms LVDT excitation. The LVDT excitation frequencies are programmable by selecting one of various jumper configurations at the power supply. To eliminate beat frequency development between channels, the two strake channels were given different LVDT excitation frequencies. As with the servoloop boards, existing FCC power supplies were used to eliminate development costs. The power supply modules, servoloop boards, and failure-detection boards were housed in a locally manufactured enclosure (fig. 9). The box was mounted in the radome aft of and between the strake actuators.

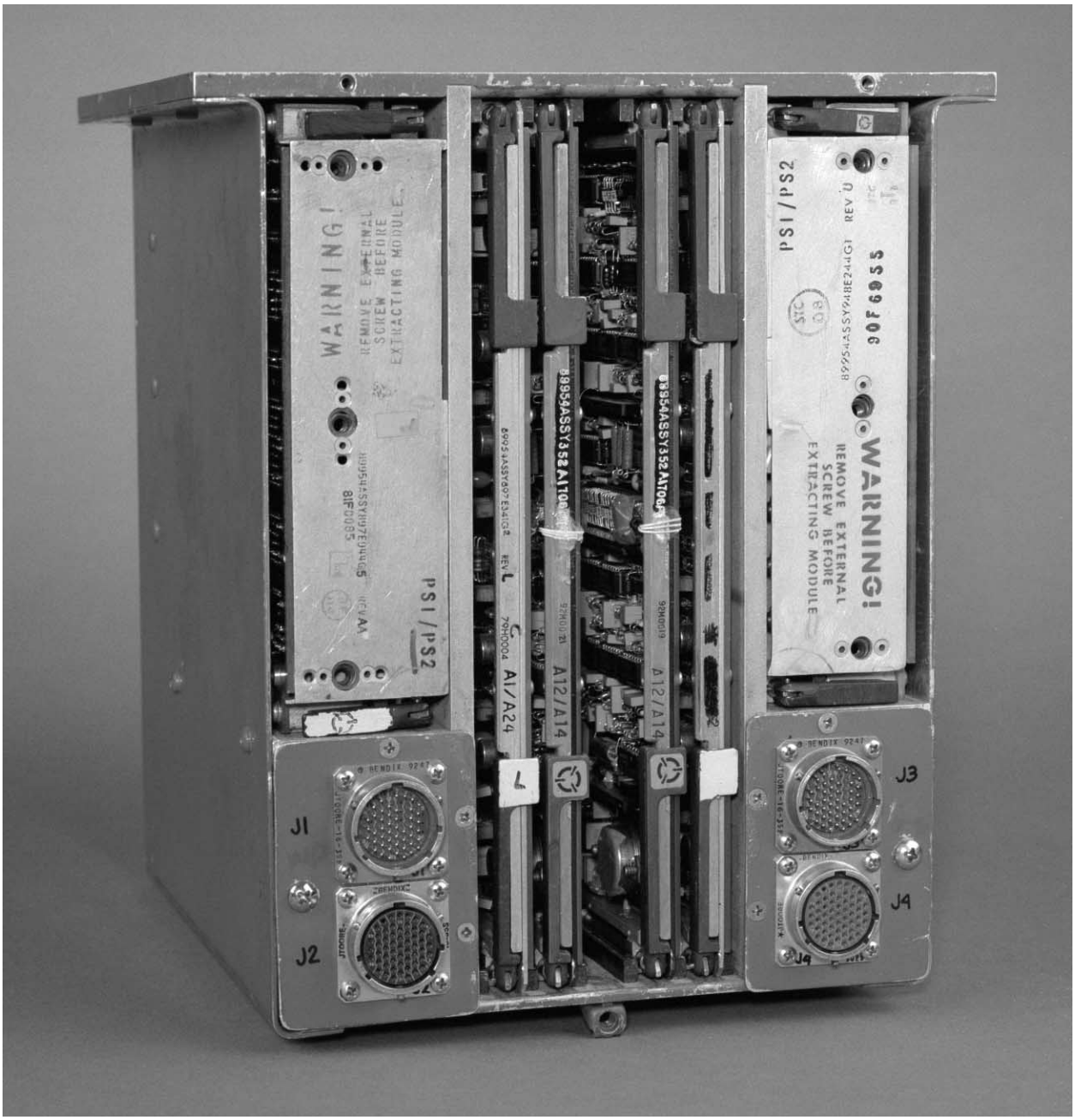

Figure 9. Power supply modules, servoloop boards, and failure-detection boards.

The design goal for the strake control system was fail-operate/fail-safe. The fail-safe mode placed the affected actuator into trail-damped mode, in which the actuator shutoff valves are opened, causing hydraulic fluid to bypass the main ram. The surface then floats freely, thus not generating a forcing moment on the aircraft. However, testing showed that the airflow over the strake did not generate enough force to overcome the breakout force and friction of the strake actuator and linkage while in trail-damped mode. Thus, the strake was essentially stuck in its last position. Evaluations of a stuck strake conducted in the DFRC F-18 simulation showed that an unrecoverable departure could occur at angles of attack of 50° or higher with a strake fully deployed.

This discovery led to implementation of a pilot-initiated system to bypass the control system and force the strakes to the fully retracted position in the event of a stuck strake. A switch added to the cockpit provided power to four independent relays which overrode the shutoff valves and commanded the actuators to fully retract independent of the control system commands. Figure 10 shows this logic.

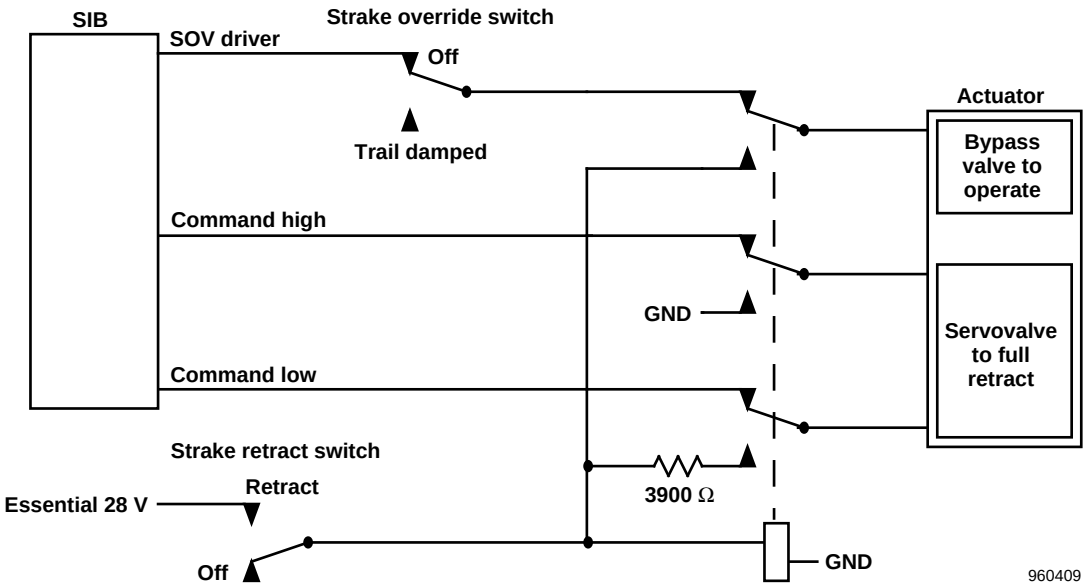

Figure 10. Strake retract system.

Cockpit modifications to accommodate the strake system were minimal. In addition to the strake retract switch, two toggle switches were added to initiate the BIT logic. Two override switches were also added to manually interrupt the shutoff valve driver signal and place the actuators in the trail-damped mode. The override switches were only used in ground operations although no measures were taken to prohibit their functionality in flight. A failure indication was added to the warning light panel to indicate any failures in the system. Display modifications that required updates to the mission computer (MC) software included the addition of a mode transition button and a gain select button to the FCS display on the DDI and a mode and gain set display on the head-up display (HUD). Figures 11 and 12 show the DDI and HUD symbologies. The onboard augmented vehicle (OAV) engagement button and maneuver selections button for the onboard excitation system (OBES) were already present from phase 2 of flight test. The FCS DDI page was used to select ANSER modes, dial-a-gain settings, OAV maneuvers, and OBES engagement. The HUD was used to display RFCS engagement, OBES engagement, ANSER modes, and dial-a-gain settings. No indication of strake position was presented in the cockpit.

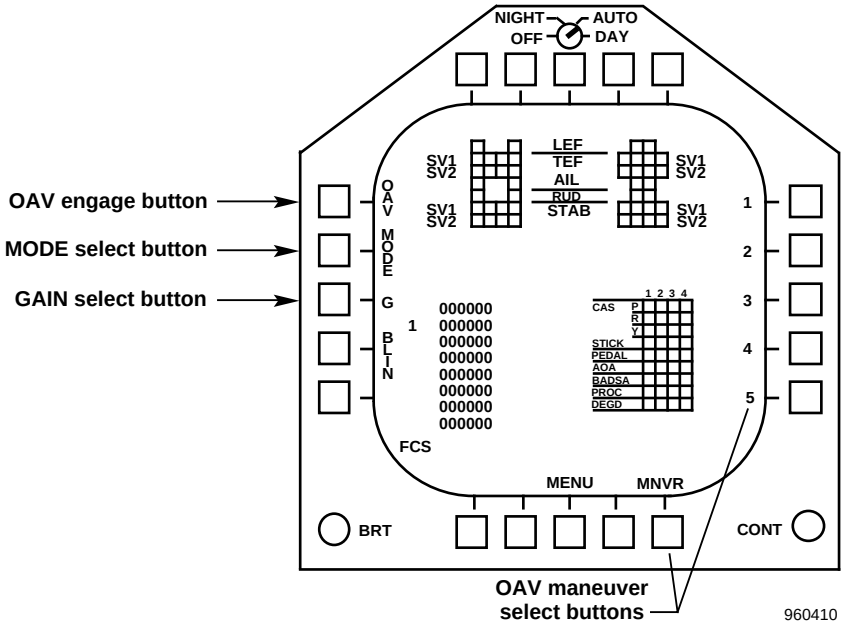

Figure 11. Flight control system display.

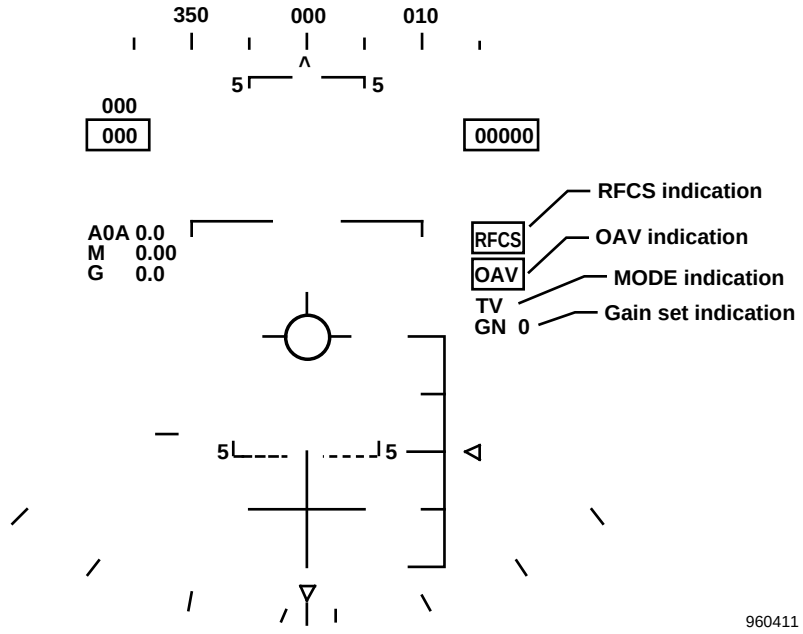

Figure 12. The HARV head-up display.

SOFTWARE DESIGN AND IMPLEMENTATION

The ANSER software was developed using two methods: hand coding from a specification and automatic code generation. The software for the ANSER can be divided into nine elements. These

elements consist of the existing shell, lateral–directional control laws, longitudinal control laws, pseudocontrols, TV mixer (ref. 4), mode logic, G-disengage, dial-a-gain, and OBES. This section discusses these software elements and design methodologies in more detail with the exception of the TV mixer.

The RFCS executes at 160 Hz in 16 minor frames; the longitudinal control laws execute at 80 Hz in the even minor frames; and the lateral–directional control laws, pseudocontrols, and TV mixer execute at 80 Hz in the odd minor frames. Each minor frame is 6.25 msec long with the requirement that the RFCS commands to the processor be computed by the 2.2-msec mark. These 2.2 msec were the critical throughput requirement. Read-only memory (ROM) was also a concern. The RFCS had only 32 kilobytes of electrically erasable programmable read-only memory (EEPROM).

Hand-Coded Software

The ANSER control law software was designed and developed from the HARV ANSER control law specification written by the Vehicle Dynamics and the Dynamics and Controls Branches of LaRC. Existing RFCS software was used as a baseline for the ANSER control laws (ref. 5). The control law software was removed, and the existing shell containing the multirate structure, disarm–disengagement logic, gross thrust estimator, and RFCS I/O software was retained (fig. 13). The TV portion of the ANSER control laws was implemented and flown first independently from the strake interfaces, followed by the complete ANSER control laws.

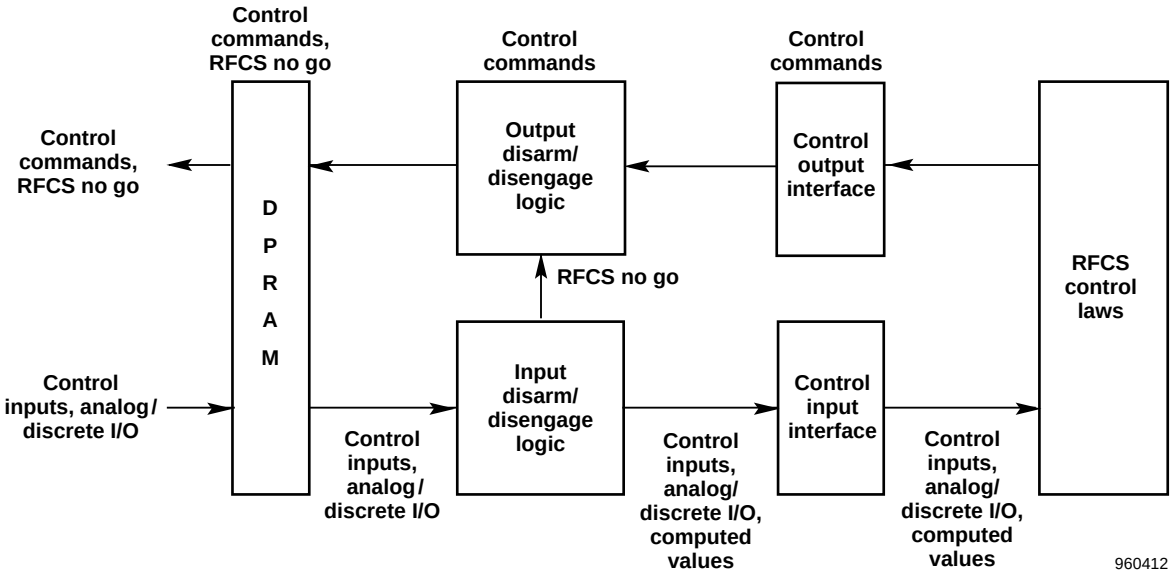

Figure 13. The RFCS shell.

Because of limited memory and throughput of the RFCS, the code was periodically reworked to reduce the amount of memory it used. To reduce the risk of throughput problems, the software

was written as efficiently as possible. The multirate structure only processed inputs at the rate and frame at which they were updated. Airdata and inertial navigation system (INS) angles were input at 20 Hz. Angle of attack (AOA) and angle of sideslip rate ($\dot{\beta}$) inertial were input at 40 Hz. Although pilot commands and rate and acceleration feedbacks were input at 40 and 80 Hz, the 40 Hz signals were processed at 80 Hz and averaged to provide continuous data to the control laws. Only processing required to compute command outputs was completed in the critical first 2.2 msec. All other computations were processed after completion of the command output computation but before the 6.25 msec end of frame.

Using the horizontal block diagrams provided in the control law specification, a control law input listing was generated to verify that the required inputs were available to the control laws. Next, each axis was modularized, and data flow paths were determined. Figure 14 shows an example of a data flow path diagram. Once the data flow was determined, the execution order of the modules was easily determined based on the data flow. The execution order ensured that outputs were computed before being used as inputs to other portions of the system. Once the data flow, execution order, computation rates, input availability, and software modularity were determined, the software was coded. The review process at the code level consisted of informal code reviews and limited module level and end-to-end testing. The module level and end-to-end testing were performed using the RFCS source code on a workstation.

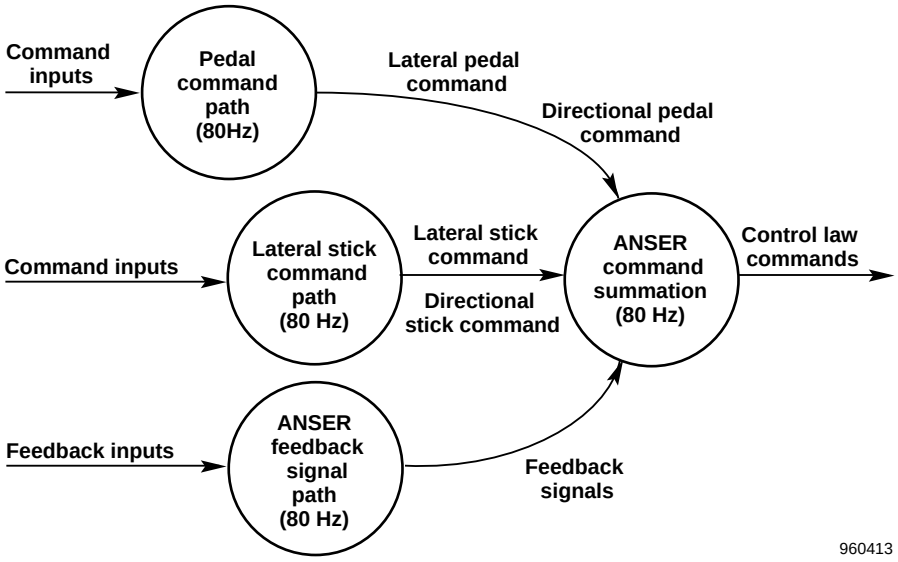

Figure 14. Lateral–directional control law data flow.

Automatic Code Generation

In developing the ANSER control laws specification, LaRC extensively used computer generated software code in both FORTRAN and Ada using MATRIX$_X$.® Using automatic code

®MATRIX$_X$ is a registered trademark of Integrated Systems, Inc., Palo Alto, California.

generation reduced the time required to make changes to the control law and to evaluate the changes in simulation, thus shortening the time required between control law modification and flight test.

The FORTRAN from the automatic code generation was used in the LaRC simulations and in the DFRC batch simulation. When changes were made to the control laws, software was regenerated using the automatic code generator and interfaced to the simulations. Check-case scripts and time histories were also provided for use in verifying the implementation. This procedure offered considerable savings in time over the traditional process of hand-coding the changes, evaluating them, and then providing the changes to programmers in the form of block diagrams to be hand-coded in that simulation. Of course, small changes, such as changing the values of a few variables, were still completed by hand directly in the code.

To complete this process of automation, carrying the automatic code generation all the way to flight was desired. Some obstacles were in this path, however. The automatically generated code was not as efficient as hand-coded software in terms of execution speed and memory. This obstacle was serious because the RFCS was operating near capacity in memory and execution time. Second, the software generation tool did not include a multirate capability. In spite of these obstacles, it was decided to use the automatically generated code for the pseudocontrols portion of the lateral–directional control law to run in the RFCS. The automatically generated code for the pseudocontrols was modified to accommodate the differences between the simulations and the RFCS.

Mode Logic

Because the ANSER control laws had three separate control law modes (TV, STV, and S), allowing in-flight selections of these modes was required. A mode selection system was, therefore, incorporated into the RFCS. Thrust vectoring was selected as the default mode; therefore, whenever RFCS was not engaged, the controls laws were in the TV mode. In addition, upon RFCS engagement, the TV mode was selected. Transitions to the STV and S modes were performed through a single mode select button on the FCS page on the DDI. A single button was used because of memory constraints in the MC. The pilot uses this mode select button to toggle through the modes, TV $\rightarrow$ STV $\rightarrow$ S $\rightarrow$ TV (fig. 15). These modes were then displayed on the HUD and downlinked to the control room.

Because a 1- to 2-sec fade existed between the modes, the HUD mode indication would be “X” so that the pilot was aware that a mode transition was in progress. The RFCS disengages requests through the paddle switch functioned from any mode. A strake failure indication from the SIB would force a mode transition back to the TV mode. Early in the design the decision to allow the pilot to remain in TV following a strake failure was made. The TV can provide greater control power to recover from abnormal conditions that might occur when recovering from a strake failure. This failure indication was latched in the RFCS software so that the failure reason could be determined in the control room before the pilot was allowed to reselect a strake mode. To limit the

aircraft to benign flight conditions during mode selections, the listed mode transition limits for TV → STV and STV → S were defined in the software as done for RFCS arming.

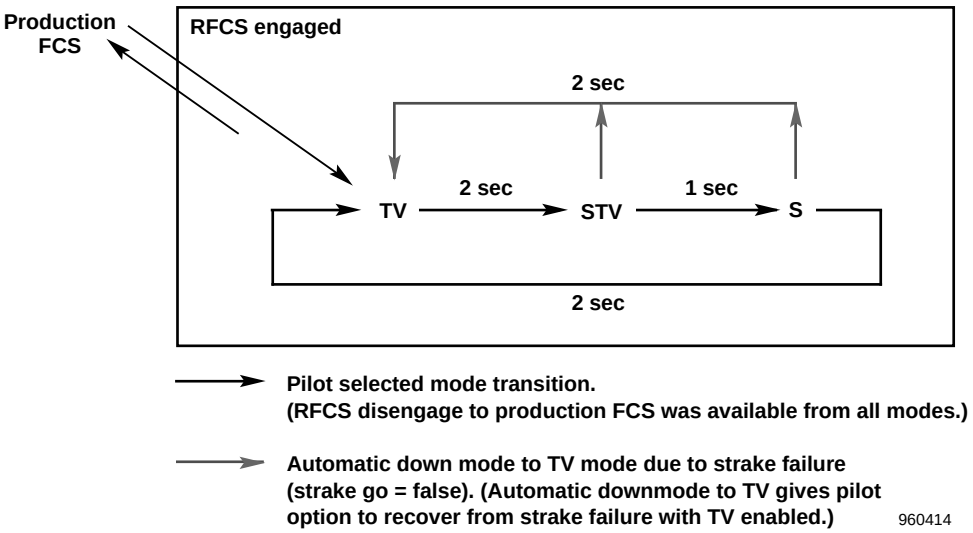

Figure 15. The ANSER mode transitions.

Table 1 lists the mode transition limits. The limit on AOA was a place holder in the software in case a smaller limit was desired. For S → TV transitions, these limits were set at or near maximum sensor values to allow the pilot to select the TV mode throughout the RFCS envelope.

Table 1. Mode transition limits.

Signal	Limit
Roll rate	< ±30°/sec
Pitch rate	< ±15°/sec
Yaw rate	< ±15°/sec
Lateral acceleration	< ±0.5 *g*
Normal acceleration	> –1 *g* or < 2 *g*
Angle of attack	< ±360°
Sideslip rate inertial	< ±5°/sec

OBES and Dial-A-Gain.

Although not new for ANSER, the OBES was used extensively during ANSER research flights. The OBES portion of the RFCS software was originally designed as a structural mode excitation system, but it has evolved into a multidisciplinary, on-aircraft test facility. The

growing number of useful applications includes aerodynamic measurements and flow visualization, parameter identification, control law evaluation, in-flight control law variability, handling qualities and inner loop stability analysis, simulation model verification, and ground test of new aircraft systems.

The initial set of research TV control laws required active in-flight structural mode excitation. This requirement resulted from marginal aeroservoelastic stability analysis predictions. Different excitation concepts were considered. An external mechanical excitation system was not selected because of its intrusive nature and integration difficulties. Another concept considered was to use the remotely augmented vehicle (RAV) facility. The RAV facility has been a critical test facility at DFRC for remote maneuver guidance, control augmentation, and remote piloting. This facility could be used to up-link an excitation signal to the aircraft which would then need to be received, processed and passed to the RFCS. The signal would then be summed to the desired control surface command. By driving the selected control surfaces at varying frequencies, the structural modes of the aircraft could be excited. The frequencies of the structural modes of interest were well within the bandwidth of the F-18 actuators.

The OBES was created by adapting this latter concept. Taking advantage of the imbedded and programmable RFCS, the functions of the RAV facility were effectively brought onboard the aircraft. With this OBES configuration, the RAV functions were performed internal to the aircraft, thus eliminating the problems associated with the remote facility. Some of the problems addressed include the up-link and down-link range and dropout problems, on-aircraft receiver requirements, signal processing, redundancy management, and time delay. Other RAV drawbacks eliminated by the OBES include the need for manpower support during the flights as well as dependence on a complex system of hardware and software.

The OBES generates the desired function and sums the signal to the desired RFCS control law path (fig. 16). The function generation logic and signal superposition are performed within the RFCS Ada software, and the selected OBES function identifier is down-linked to the control room for test point verification. For these flight test points, the test pilot would simply initiate the appropriate OBES maneuver and maintain flight conditions. The OBES performs the selected maneuver.

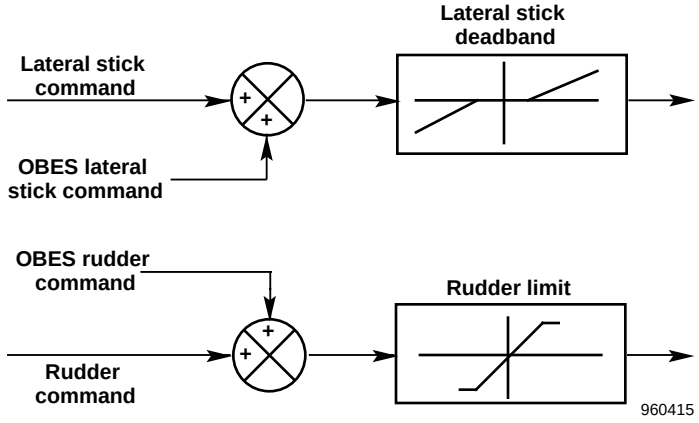

Figure 16. The OBES command summation examples.

For ANSER flight testing, the OBES was used for nose strake aerodynamic measurements and flow visualization, nose strake loads flight clearance, closed- and open-loop parameter identification and nose strake preflight built-in test excitation.

A dial-a-gain capability was added to the RFCS to add flexibility to the flight test of the ANSER control laws. The option of eight separate gain set selections was made available. For ANSER, three gain sets were defined for the longitudinal axis with one gain set defined as a default, baseline set. These gain sets were selected through the cockpit DDI, and the current gain set was displayed on the HUD and down-linked for control room monitoring. Gain selection was allowed throughout the flight envelope before or after RFCS engagement; however, with any RFCS disengagement, the selected gain set defaulted back to the baseline gain set.

g-Disengage

The RFCS and Ada software were originally intended to be a class B system to reduce the software testing and verification requirements (ref. 3). Although many definitions of class B exist, in general this designation meant that an error in the RFCS or software could not result in loss of aircraft.

Vehicle modifications required by the installation the TVCS and ANSER systems added a significant amount of weight at the extreme fore and aft ends of the aircraft. Because of this “flying dumbbell” configuration, expected load levels in the forward fuselage area during maneuvering flight were significantly increased. Structural analysis indicated that a reduction in symmetric and asymmetric maneuvering load limits was required (table 2). Software modifications to enforce the new limits could not be made to the basic flight control system, so a flight operations limit was imposed.

Table 2. Production F/A-18 and HARV load limits.

Load limit	Production F/A-18	HARV
Symmetric	–3.0 *g* to 7.6 *g*	–2.0 *g* to 5.4 *g*
Asymmetric	0 *g* to 6.0 *g*	0 *g* to 4.2 *g*

Although the flight operations limit specifically restricts the pilot from maneuvering above the symmetric and asymmetric load limits, the aircraft still has the command authority and control power available to significantly exceed the aircraft structural limits in the lower right-hand corner of the RFCS envelope (h = 15,000 ft, M = 0.7). During software testing, it was found that hard-over stabilator commands from the RFCS could not be countered by the pilot in enough time to prevent an over-*g*. As a result to balance the risk of an undetected RFCS software fault with the general desire to design and test in a class B environment, a function to predict and reduce the possibility of an over-*g* was implemented in the RFCS.

This function, called the *g-disengage*, was only active at high dynamic pressures where an over-*g* was possible. Structural loads in the critical forward fuselage area were estimated from flight control accelerations and rates and projected ahead in time with a lead filter. When the projected load exceeded the computed load limits, the RFCS stayed engaged. However, the RFCS stabilator command was ignored, and the stabilator was driven to the basic F/A-18 stabilator command. Once the stabilator got within 5° of the basic system stabilator command, the RFCS was disengaged. In this way, the *g*-disengage reduced the potential of an over-*g* caused by a failure in the RFCS. It dynamically limited the stabilator commands.

Once the *g*-disengage software was implemented, it was complied and stored in a designated portion of the EEPROM. This designation was done so that when software updates were made, a bit-for-bit comparison could be completed using the previous version of *g*-disengage. This comparison ensured that any software updates to the RFCS did not affect the *g*-disengage portion of the software.

SYSTEM INTEGRATION AND TESTING

The ANSER system was extensively tested before it was integrated into the aircraft. Testing was broken into four levels: card level testing, box level, integrated system, and system validation. The designer performed card level testing to check the design and build of the card. Each card was tested against the design as much as possible. The chassis wiring was also tested at this level. Box level testing was a more intensive test and was integrated with an actuator and an actuator model. Integrated system testing included the FCS and the actuators or actuator models. System validation testing included the actuators or actuator models, FCC, and closed-loop simulation of the vehicle dynamics.

An actuator model was developed for the integration and testing of the strake system. The strake actuator model was designed to accurately model the response of the forebody strake actuators in software. The model receives strake commands as inputs from the SIB and hinge moment from the simulation, and this mode gives out the spool and ram positions, voltages, and ram velocity as outputs to the SIB and then as outputs to the simulation. The actuator model calculates spool and ram positions in normal operational mode or in trail-damped mode. The models are implemented on a Versa Model Eurocard (VME) system which operates at 800 Hz.

Box level testing checked the box and actuator interfaces. A function generator replaced the FCC and provided the command voltages to the interface box. The initial tests verified the interface box under steady-state conditions. A voltage was applied, and the actuator or actuator model position was verified. Once the steady-state inputs were evaluated, a full-scale ramp input was then used to evaluate the time history of the interface box and of the actuator and actuator model. After the ramps, a frequency response test was run to verify the dynamics of the servoloop. Failures were then introduced while a ramp was input to verify that the failure-detection circuits operated as expected. Table 3 indicates the failures that were introduced and in what level of testing these failures were performed. After the failure-detection tests were run, BIT was tested, and failures were introduced to verify that the implementation detected the failures properly.

Table 3. Integration testing matrix.

Failures	Card level	Box testing	Integrated system	System validation
Ram position, high open	Yes	One channel Two channels with actuator and actuator model	One channel Two channels	One channel Two channels
Ram position, low open	Yes	No	No	One channel Two channels
Spool position, high open	Yes	One channel Two channels with actuator and actuator model	One channel Two channels	One channel Two channels
Spool position, low open	Yes	No	No	One channel Two channels
FCC command to strake interface box, open	Yes	One channel Two channels with actuator and actuator model	One channel Two channels	One channel Two channels
Strake interface command to actuator or actuator model, open	No	One channel Two channels with actuator and actuator model	One channel Two channels	One channel Two channels
LVDT excitation, open	No	One channel Two channels with actuator and actuator model	One channel Two channels	One channel Two channels
Pressure discrete, open	Yes	One channel Two channels with actuator and actuator model	One channel Two channels	One channel Two channels
Power, open	Yes	One channel Two channels with actuator and actuator model	One channel Two channels	One channel Two channels
Shut off valve, open	Yes	One channel Two channels with actuator and actuator model	One channel Two channels	One channel Two channels
Servocurrent, open	Yes	One channel Two channels with actuator and actuator model	One channel Two channels	One channel Two channels

Three major anomalies were discovered during box level testing. First, a grounding problem required the addition of a second 1.832-MHz clock instead of relying on a single clock to drive both servoloop boards. Second, a sign error was discovered in the spool position versus command current algorithm, requiring minor redesign. Third, the counter used to step through the BIT sequence would intermittently reset or arbitrarily jump to a different test. Troubleshooting revealed a shared ground between the digital BIT circuitry and the analog circuitry on the failure-detection board. This problem was documented but was deemed a nuisance. No fix was implemented, so the problem was carried through to the aircraft and often required multiple BIT operations before each flight.

Integrated system testing was the next level. The RFCS provided the ability to program the OBES to generate identical ramps and square waves as those from the function generator. The tests which had previously been performed during box level testing were repeated with the interface box, actuator or actuator model, and FCC integrated. The only discrepancy noted during system integration testing was a lack of fidelity in the strake actuator model. This model was improved and testing continued.

Upon completion of integrated system testing, system level validation was run. A high-fidelity simulation of the vehicle dynamics was integrated with the interface box, FCC, and actuators or actuator models. The flight software was installed in the RFCS, and testing similar to that performed in the integrated systems testing was performed (table 3). Time histories, frequency responses, and induced failures were run at various flight conditions. The MC modifications, RFCS, and total system were validated. This validation included displays and switchology as well as failures, mode transitions, time histories, and frequency responses. During validation testing, a single failure in the FCC command to the SIB would result in the actuator trying to respond to both commands simultaneously. Both channels' servovalve commands versus spool position monitors would fail, placing the actuator in trail-damped mode. This single point failure combined with the discovery that trail-damped is an unacceptable failure mode, resulted in developing and implementating the strake retract system.

Additionally certain conditions, such as a single failure in a main ram LVDT signal, could cause a failure in the second channel. Such failures also resulted in the trail-damped mode. Troubleshooting revealed that the failure in the first channel ram position drove the command current in the partner channel higher momentarily to compensate. The servoposition versus command current monitor failure discrete would momentarily trip and then self-reset. This transition typically lasted 20 to 25 msec. The optical relay which controls the actuator shutoff valve is specified to recover from transitions in less than 50 msec. That relay would latch to a failed state and could not be reset because of the design decision not to include a manual reset.

Aircraft integration testing was fairly limited because of high confidence in the simulation implementation. Testing consisted of time histories in the three RFCS modes. Open wire failures were induced to verify failure-detection, and cockpit functions were verified. The only known anomaly was the BIT problem discovered during integration testing.

RFCS VERIFICATION

With the implementation of the *g*-disengage software, the class B designation of the rest of the RFCS software was used to define the level of verification testing required before flight. Independent testing has shown that the RFCS envelope limits and the OBES are the only elements of RFCS which affect flight safety.* Since those tests, the vane load limiting was also determined to affect flight safety. With this affect in mind, the ANSER verification testing requirements were defined. The RFCS envelope limits (15,000 ft < h < 45,000 ft, M < 0.7) were verified. A bit-for-bit comparison of the *g*-disengage software was performed to verify that *g*-disengage executable did not change from a previously verified version. The RFCS software configuration identifier was verified to ensure that the software release identification was correct. Thrust-vectoring vane system (TVVS) command limiters were verified in the lower right- and left-hand corners of the envelope. Because the OBES could also affect safety of flight, each OBES maneuver was flown at flight conditions starting in the lower right-hand corner of the envelope to determine where in the flight envelope the individual maneuver affected flight safety. Once this determination was completed, a flight operations limit was defined for that maneuver. Although some informal testing was performed to gain confidence in the operation of the software, no other RFCS software testing was required. Any errors existing in the software were considered to be only mission critical. The project decided to accept this risk knowing that a complete verification would take an unreasonable amount of time.

FLIGHT TEST MONITORING

Flight test monitoring of the RFCS and the processor FCS for phase 2 was done on two control room display pages. An FCS display page was designed to look similar to the FCS DDI display in the aircraft (fig. 17). This page displays leading-edge flap, trailing-edge flap, aileron, rudder, stabilator and TVV position and failure status; lateral stick, longitudinal stick and rudder pedal positions, and failure status; and FCS analog and discrete I/O failure status. The RFCS display page was used to monitor the RFCS I/O and system functionality during RFCS engagement (fig. 18). Aircraft rates, accelerations, AOA, and rates of change in angles of attack and sideslip, $\dot{\alpha}$ and $\dot{\beta}$, were displayed with RFCS arm and RFCS engage–disengage limit windows. The TVVS commands and positions were displayed with maximum limits. The RFCS Mach number and altitude were displayed with RFCS envelope limits incorporated. Engine parameters included power lever angle (PLA), nozzle area, turbine discharge pressure, and gross thrust. The RFCS abort and fail-to-arm flags were also displayed. The TVVS temperatures and aircraft loads as a function of percent of maximum allowable were also displayed to allow for the option of not having a structural loads engineer in the control room.

*Earls, M.R., "Nasty RFCS Test Report," HA92-84-601, 1992. (This report is an unpublished working paper and is not available to the public.)

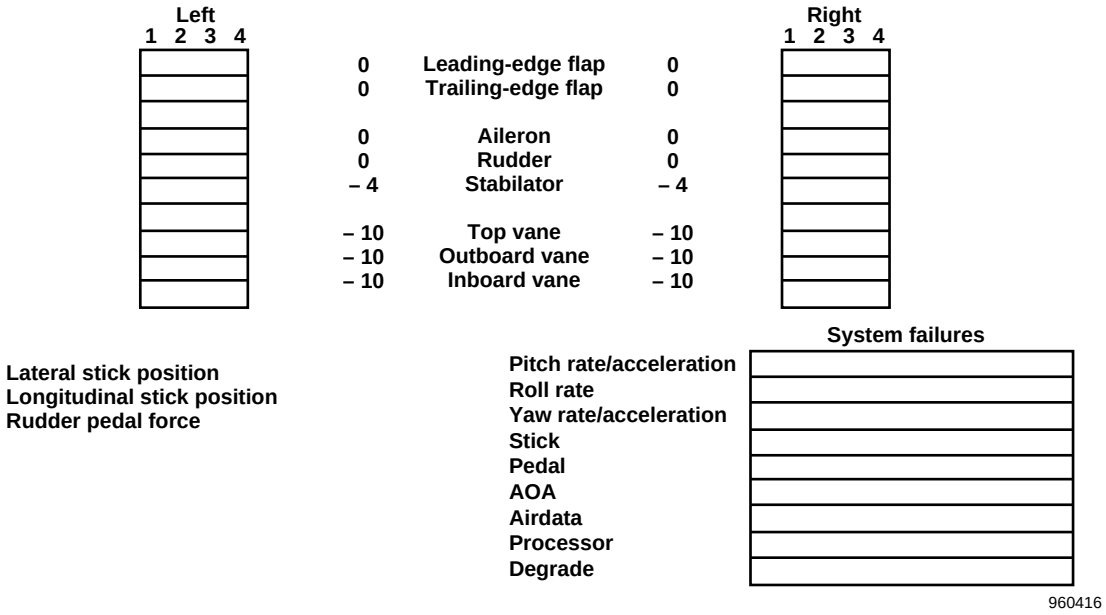

Figure 17. The HARV RFCS monitoring page.

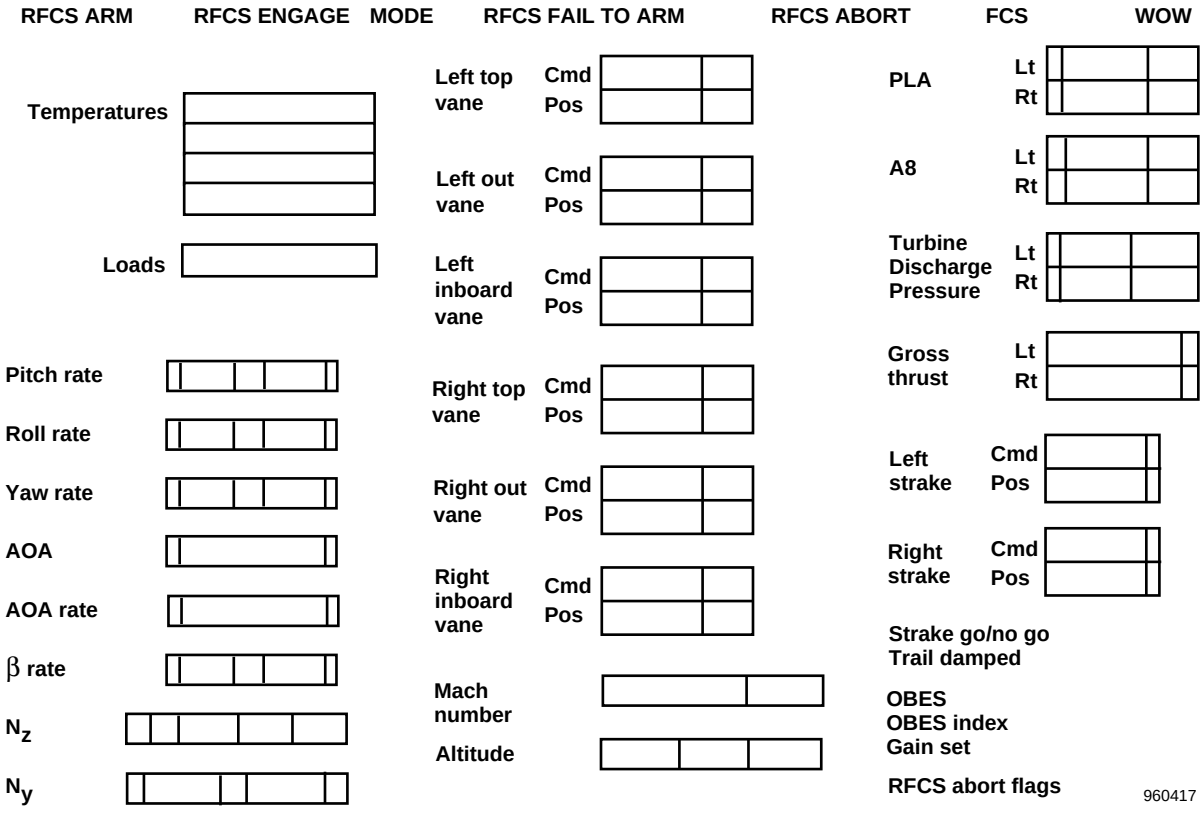

Figure 18. The RFCS monitoring page.

In addition to the existing RFCS and FCS display pages used on phase 2, other parameters were incorporated into display pages for the phase 3 (ANSER) portion of flight test. A new ANSER parameter display system (PDS) display page was designed for monitoring strake actuator commands versus actuator positions, servocurrents, spool positions, and failure-detection circuitry during flight (fig. 19). A BIT index was displayed for preflight BIT monitoring. The strake go flag, ANSER mode (TV, STV, S), trail-damped indication, FCS caution, and strake retract switch position were also displayed. The FCS caution was displayed to alert the systems engineer that an FCS problem existed. The systems engineer could then display the FCS display page to troubleshoot the FCS problem. The RFCS display page was modified for phase 3 to include ANSER mode, strake command, strake position, strake go flag, and current gain set selected. To indicate an ANSER mode transition (for example, TV $\rightarrow$ STV) to the systems engineer, the ANSER mode would flash at approximately 5 Hz during the transition (figs. 18–19). Some of the more critical parameters, such as ANSER mode, trail damped, and strake go, were displayed on the ANSER PDS and the RFCS display pages. This combination display reduced the systems engineer's scan during flight test when critical calls to the test pilot, flight controller, or both, were required. To isolate possible RFCS anomalies from SIB anomalies, the RFCS page displayed command and position data from the SIB, and the ANSER PDS page displayed command and position data from the SIB.

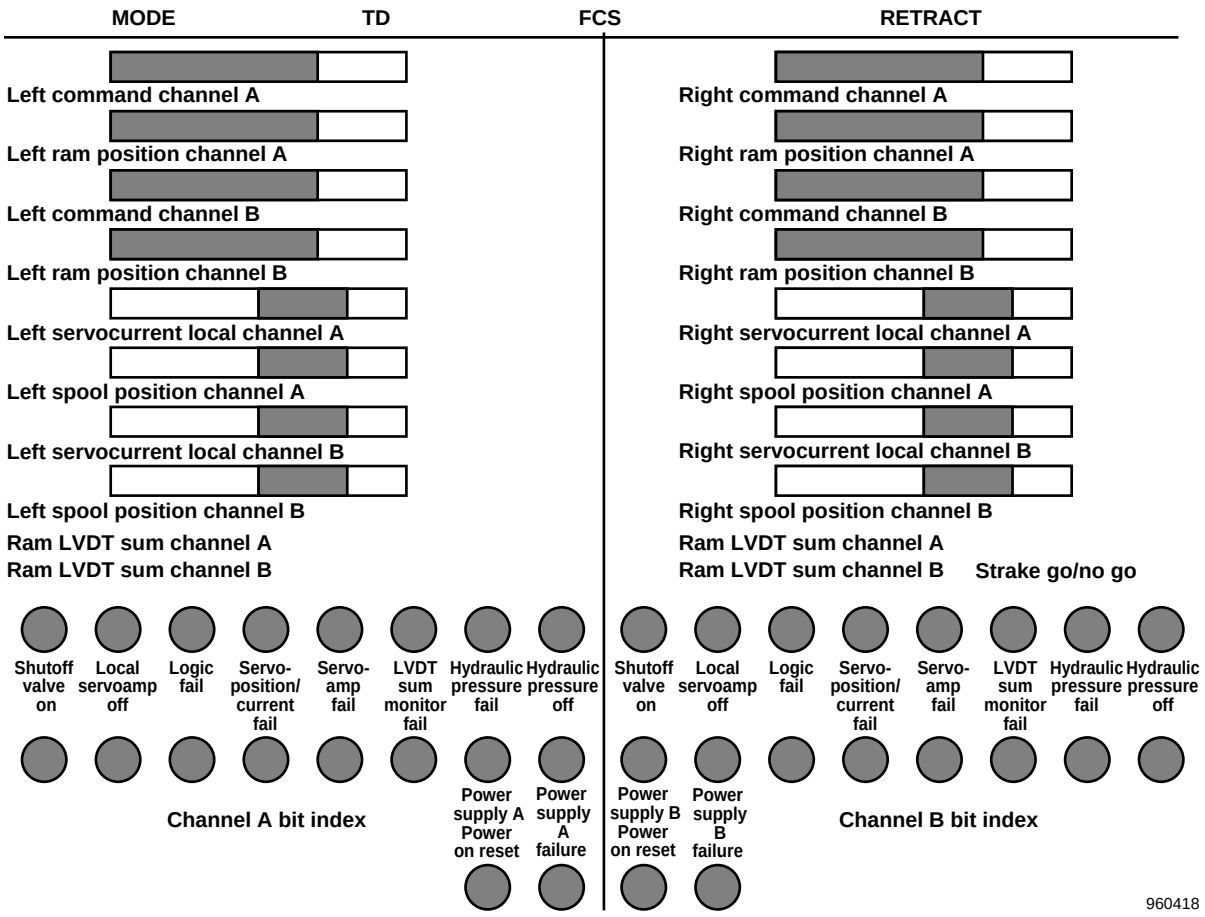

Figure 19. The ANSER PDS page.

FLIGHT TEST RESULTS

The ANSER system was installed and flown for the final 89 flights of the HARV flight program. With one exception, flight performance of the system was generally successful. The servoposition versus command current test would fail and self-reset during large amplitude lateral–directional maneuvers in the 30° to 50° angle-of-attack range. Typically, one channel of one actuator would indicate a failure. Troubleshooting revealed a divergence in the RFCS command to the servoloop between the two channels of the affected actuator. The two independent servoloops would command a different servovalve position based on the FCC commands. The servovalve would respond to a position midway between the two commands. When the commands diverged sufficiently, the failure-detection algorithm would declare a failure (fig. 20). The test tolerance was increased to allow the commands to differ by 8.5° or nearly 10 percent of full scale. This increase reduced the frequency of the failures, but it did not eliminate them completely.

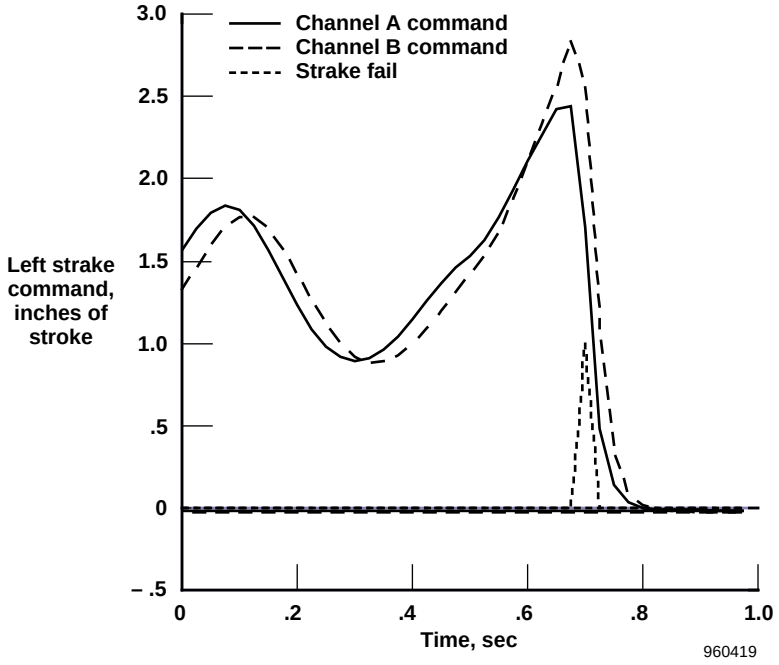

Figure 20. Example of in-flight command miscomparison.

Investigations into the cause of the divergent FCC commands are ongoing. The RFCS channels appear to be receiving different values for lateral stick commands resulting from the quad signal selection algorithm in the FCC. The high gain nature of the RFCS control laws amplifies this difference and results in the different strake commands. Documentation of these findings is hindered somewhat because internal FCC data are only available on two of the four channels through the MIL-STD-1553 data bus. Project scheduling concerns prohibited a resolution of this problem; therefore, a set of research data in the flight regime affected was not obtained. The probable fix would have been a persistence counter in the RFCS on the strake go discrete. These failures were

generally one or two frames in length. A five-frame persistence on the strake go discrete would have allowed the S or STV mode to remain engaged while the failure self-reset.

Other problems encountered in the flight program were minimal. An integrated circuit failure occurred causing loss of one flight for repair. A failed spike suppression diode in an unrelated system caused corruption of strake power. This diode failure resulted in an self-start of the ANSER BIT logic in flight. The retract system was used, and the aircraft was recovered normally.

LESSONS LEARNED

Several lessons were learned in the development of the ANSER system. These lessons can be applied to future system integration efforts. An assumption was made early in the program that placing the actuators to trail-damped was an acceptable failure mode. This assumption drove a great deal of the system design and eventually proved false. A substantial effort was then required to implement the strake retract system. Had the assumption been disproved earlier in the design phase, the normal failure mode could have been to a strake-closed configuration.

The decision to have failures automatically reset was adequate in the majority of cases, but when a main ram LVDT failure occurred, the partner channel servocurrent versus spool position monitor failed and reset faster than the electronics could recover. This rapid automatic reset resulted in an unresettable trail-damped condition. The addition of a manual reset capability along with the automatic reset would have alleviated this problem.

Monitoring the preflight built-in test manually rather than automatically proved to be a valid approach for this application. This monitoring eliminated the development of a processor-based system to perform this function.

A persistence counter on the strake go discrete may have prevented the reversions to TV mode in the 30° to 50° angle-of-attack range during the flight phase. Additionally, a cross-channel comparison of RFCS parameters may have detected the command miscomparisons, and a routine could have been implemented to average these signals.

In the RFCS area, increased throughput and ROM would have eased the software design. Streamlining the code a great deal was necessary to accommodate these limitations of the RFCS.

CONCLUDING REMARKS

A system to enhance high-angle-of-attack flight handling qualities was developed by NASA Langley Research Center and integrated into the F-18 High Alpha Research Vehicle by NASA Dryden Flight Research Center. The actuated nose strake for enhanced rolling system proved reliable throughout 89 test flights. This system consists of two actuated control surfaces installed on a specifically constructed radome.

Actuator control was performed by a strake interface box with commands generated by the control laws residing in the research flight control system (RFCS). These control laws consisted of three modes: thrust vectoring (TV), strakes and thrust vectoring (STV), and strake (S). The TV mode uses the TV system for longitudinal and lateral–directional control. The strakes are not commanded in this mode. The system reverts to the TV mode in the event of a strake failure. The STV mode uses TV for longitudinal control and a combination of strakes with TV for lateral–directional control. The S mode uses TV for longitudinal control and strakes for lateral–directional control. The RFCS also resides in the onboard excitation system and allows open- and closed-loop functions to be summed into the RFCS control laws for research flexibility.

Extensive testing was performed to qualify the system for flight. This testing revealed one major and several minor system problems. The major problem was that the failure mode for the system which had been designed to place the failed strakes in trail-damped mode was inadequate. This inadequacy could result in a out-of-control situation. This problem resulted in the implementation of a manually activated retract system to close the strakes if a trail-damped situation occurred.

In the 30° to 50° angle-of-attack range, strake commands would differ between the two flight control channels driving a particular strake. This difference resulted in a reversion to TV mode. A correction was not implemented, and a portion of the flight research program was not completed because of this failure. With this exception, the program was generally successful, and the majority of the research objectives were met.

REFERENCES

[1]Gera, Joseph, "Flight Test Status of the NASA High-Angle-of-Attack Technology Program," *High-Angle-of-Attack Projects and Technology Conference Proceedings*, NASA CP-3137, 1992.

[2]Murri, D.G., Shah, G.H., and DiCarlo, D.J., "Preparations for Flight Research to Evaluate Actuated Forebody Strakes on the F-18 High-Alpha-Research Vehicle," *Fourth High-Angle-of-Attack Technology Conference Proceedings*, NASA CP-10143, 1994.

[3]Chacon, Vince, Pahle, Joseph W., and Regenie, Victoria A., *Validation of the F-18 High Alpha Research Vehicle Flight Control and Avionics System Modifications*, NASA TM-101723, 1990.

[4]Bundick, W. Thomas, Pahle, Joseph W., Yeager, Jessie C., and Beissner, Fred L., Jr., *Design of a Mixer for the Thrust-Vectoring System on the High-Alpha Research Vehicle*, NASA TM-110228, 1996.

[5]Regenie, Victoria A., Earls, Michael, Le, Jeanette, and Thomson, Michael, *Experience with Ada on the F-18 High Alpha Research Vehicle Flight Test Program*, NASA TM-104259, 1992.

REPORT DOCUMENTATION PAGE

Form Approved
OMB No. 0704-0188

1. AGENCY USE ONLY (Leave blank)	2. REPORT DATE	3. REPORT TYPE AND DATES COVERED
	October 1996	Technical Memorandum

4. TITLE AND SUBTITLE

Design and Integration of an Actuated Nose Strake Control System

5. FUNDING NUMBERS

WU 505-68-30

6. AUTHOR(S)

Bradley C. Flick, Michael P. Thomson, Victoria A. Regenie, Keith D. Wichman, Joseph W. Pahle, Michael R. Earls

7. PERFORMING ORGANIZATION NAME(S) AND ADDRESS(ES)

NASA Dryden Flight Research Center
P.O. Box 273
Edwards, California 93523-0273

8. PERFORMING ORGANIZATION REPORT NUMBER

H-2134

9. SPONSORING/MONITORING AGENCY NAME(S) AND ADDRESS(ES)

National Aeronautics and Space Administration
Washington, DC 20546-3191

10. SPONSORING/MONITORING AGENCY REPORT NUMBER

NASA TM-104324

11. SUPPLEMENTARY NOTES

Presented at the 5th High Angle of Attack Technology Conference, NASA Langley Research Center, Hampton, Virginia, Sept. 17–19, 1996.

12a. DISTRIBUTION/AVAILABILITY STATEMENT

Unclassified—Unlimited
Subject Category 05

12b. DISTRIBUTION CODE

13. ABSTRACT (Maximum 200 words)

Aircraft flight characteristics at high angles of attack can be improved by controlling vortices shed from the nose. These characteristics have been investigated with the integration of the actuated nose strakes for enhanced rolling (ANSER) control system into the NASA F-18 High Alpha Research Vehicle. Several hardware and software systems were developed to enable performance of the research goals. A strake interface box was developed to perform actuator control and failure detection outside the flight control computer. A three-mode ANSER control law was developed and installed in the Research Flight Control System. The thrust-vectoring mode does not command the strakes. The strakes and thrust-vectoring mode uses a combination of thrust vectoring and strakes for lateral–directional control, and strake mode uses strakes only for lateral–directional control. The system was integrated and tested in the Dryden Flight Research Center (DFRC) simulation for testing before installation in the aircraft. Performance of the ANSER system was monitored in real time during the 89-flight ANSER flight test program in the DFRC Mission Control Center. One discrepancy resulted in a set of research data not being obtained. The experiment was otherwise considered a success with the majority of the research objectives being met.

14. SUBJECT TERMS

Ada, Digital systems, F-18 High Alpha Research Vehicle, Flight control, Nose strakes, Servoloop, Servoactuators

15. NUMBER OF PAGES

31

16. PRICE CODE

AO3

17. SECURITY CLASSIFICATION OF REPORT	18. SECURITY CLASSIFICATION OF THIS PAGE	19. SECURITY CLASSIFICATION OF ABSTRACT	20. LIMITATION OF ABSTRACT
Unclassified	Unclassified	Unclassified	Unlimited